

Scanning Force Microscopy Study on a Single-Stranded DNA: The Genome of Parvovirus B19

Giampaolo Zuccheri,^[a] Anna Bergia,^[a] Giorgio Gallinella,^[b] Monica Musiani,^[b] and Bruno Samori^{*[a]}

The genome of parvovirus B19 is a 5600-base-long single-stranded DNA molecule with peculiar sequence symmetries. Both complementary forms of this single-stranded DNA are contained in distinct virions and they hybridize intermolecularly to double-stranded DNA if extracted from the capsids with traditional methods, thus losing some of their native structural features. A scanning force microscopy analysis of these double-stranded DNA molecules after thermal denaturation and renaturation gave us the chance to study the possible states that this DNA can assume in both its single-stranded and double-stranded forms. A novel but still poorly reproducible in situ lysis experiment that we have conducted on single virions with the scanning force microscope made it possible

to image the totally unpaired state that the single-stranded DNA molecule most likely assumes inside the viral particle. Structural considerations on single molecules offer the opportunity for the formulation of plausible hypotheses on the interaction between the DNA and the viral structural proteins that could prove important for the DNA packaging in the capsid and, possibly, the viral infection mechanisms.

KEYWORDS:

DNA structures · nanostructures · scanning probe microscopy · single molecules · viruses

Introduction

The genome of the B19 virus, a member of the *Erythrovirus* genus in the Parvoviridae family, consists of one molecule of single-stranded DNA, about 5600 bases in length, of either positive or negative polarity (defined by comparison with the sequence of the coding messenger RNA). One of the two complementary forms of the single-stranded DNA molecule is contained in each capsid. Positive and negative strands are packaged in separate particles in equal numbers. After extraction the complementary strands may hybridize to form double-stranded DNA.

The sequence of this genome possesses some peculiar symmetry properties. The 4830-base central part contains the frames coding for all the viral proteins; the two 383-base noncoding terminal regions have inverted sequences; furthermore, the distal 365 bases of these regions are in a nearly perfect internal palindromic arrangement (Figure 1 A).^[1] These symmetry elements could yield a number of different self-annealing schemes. In one of these, each terminal palindrome region folds back onto itself and base-pairs internally within the terminus: The two resulting paired stretches ("fold-back" ends; Figure 1 B) are very efficient priming locations for the replication of the viral genome during the infection. Alternatively, the two terminal sequences could hybridize with each other (Figure 1 C–D) forming a short double-stranded stem joined to a single-stranded loop, and this could imply that a different replicative pathway needs to be followed in this case.

To achieve a deeper insight into the structural organization and the replication of the B19 virus, which is still largely unknown, we studied the structural properties of its peculiar

genome with the scanning force microscope^[2] (SFM; also known as atomic force microscope, AFM). The SFM has already proved as a very useful instrument for the structural analysis of DNA and nucleoprotein complexes: It can image at high resolution without the need for any external contrast enhancement technique.^[3, 4]

In the experiments reported here, the single-stranded viral DNA, solubilized and separated from all the viral proteins, displayed a tendency for the intramolecular base pairing of the two terminal palindromes. On the other hand, when the lysis of single, separated virions was carried out and followed in situ, where the DNA molecules extracted from the capsids could not interact with each other, the observed single-genome molecules they contained were found in a non-base-paired state: The molecules appeared fully linear, without any hairpins or double-stranded stretches in the terminal palindromes. This state is unexpected due to the remarkable thermodynamic stability of the fully paired termini in solution as compared to the unpaired ones.

[a] Prof. B. Samori, Dr. G. Zuccheri, Dr. A. Bergia
Department of Biochemistry "G. Moruzzi"
University of Bologna
Via Imerio 48, 40126 Bologna (Italy)
Fax (+390) 512094388
E-mail: samori@alma.unibo.it

[b] Dr. G. Gallinella, Prof. M. Musiani
Department of Clinical and Experimental Medicine
Division of Microbiology
University of Bologna, Bologna (Italy)

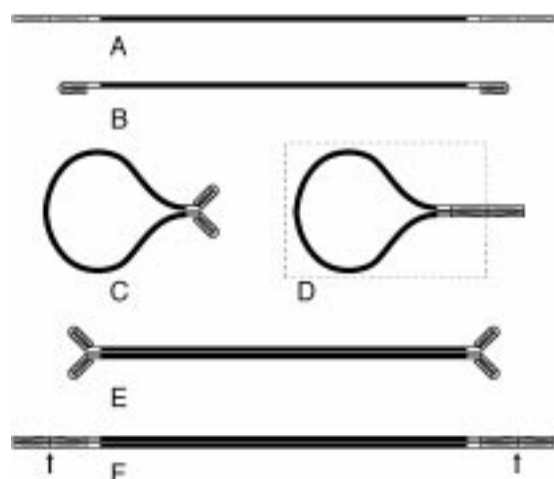


Figure 1. Schematic representation of the most significant among the possible states of B 19 DNA. A: A single-stranded molecule with extended termini. The gray stroked rectangles represent the two parts of the terminal palindromes; the white rectangle is the nonpalindromic part of the inverted sequences. B: A single-stranded molecule with double-stranded "fold-back" termini: The terminal 365 bases at both ends of the genome molecules are palindromes and can base-pair internally. C: A single-stranded molecule with double-stranded "fold-back" termini. The nonpalindromic complementary parts (white rectangles) can base-pair to form the forked termini. D: A single-stranded molecule with double-stranded extended termini. The structure inside the dashed box can be formed by BssHI-digested B 19 DNA. E: An annealed double-stranded molecule with "fold-back" termini. The apexes of the hairpins contain nonpaired bases. F: A completely base-paired extended double-stranded molecule. The arrows point to the restriction sites of BssHI (the portion between the arrows is left after digestion). The central parts of the DNA molecules (black rectangles) are not drawn to scale with respect to the tails.

Editorial Advisory Board Member:^[*]

Bruno Samori

studied chemistry at the Faculty of Industrial Chemistry of the University of Bologna. He carried out research with polarization spectroscopy techniques on liquid crystalline materials at the University of Bologna, at King's College of London with S. F. Mason, at the University of California at Berkeley with I. Tinoco, and at the University of New Mexico with C. Bustamante. In 1990 he became Full Professor of Organic Chemistry at the University of Calabria, Cosenza, and the focus of his research moved towards studies of DNA superstructures by using the scanning force microscope (SFM). After five years he returned to the University of Bologna where he is presently devoting his research to studying superstructures, interactions, and recognition mechanisms in biological macromolecules by imaging and manipulating them at the single-molecule level with the SFM and with SFM-based nanomanipulators.



[*] Members of the Editorial Advisory Board will be introduced to the readers with their first manuscript.

Results and Discussion

SFM structural analysis of purified viral DNA

The two complementary forms of parvovirus B 19 single-stranded DNA contained in different virions can hybridize to fully paired double-stranded molecules when isolated in solution with classical methods. The resulting more stable double-stranded structures assume base-pairing arrangements different from those available to the viral single-stranded DNA (see Figure 1). The purified extracted viral DNA was deposited on the surface of freshly cleaved mica and observed with the SFM.^[2] Most of the DNA molecules (92% out of 78 observed molecules) appeared in a linear form (Figure 2A): Their mean length was

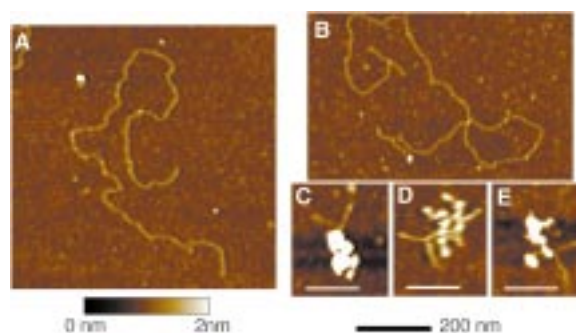


Figure 2. Tapping-mode scanning force microscopy (TM-SFM) images of purified B 19 DNA adsorbed on the surface of freshly cleaved mica before and after heat denaturation. The height data is coded in shades of color (see colorbar). A: Micrograph of a linear double-stranded molecule purified from virions. No terminal structures are evident in most of the molecules. B–E: Micrographs of heat-denatured and quickly reannealed B 19 DNA molecules: B: A linear reannealed double-stranded molecule showing forked double-stranded termini; C–E: examples of reannealed coiled single-stranded B 19 DNA presenting forked termini protruding from their compact, irregularly coiled bodies. The size bars are 100 nm long in these enlargements.

(1.86 ± 0.10) μm (mean \pm standard deviation), a value near that expected for a 5600-base-pair (bp) DNA in the B (hydrated) form (1.89 μm). A few molecules (8%) appeared with one bifurcated terminus; none of the molecules displayed two bifurcated termini (see Figure 1 E). These linear double-stranded molecules with bifurcated ends form if the intermolecular base-pairing coexists with an intramolecular folding at one or both the palindromic termini of the molecules (as sketched in Figure 1 E). The observed double-stranded forked termini had a mean length of (56 ± 14) nm, as expected for the pairing of the complementary 365 bases of the palindrome (365/2 bp, 62 nm if B-DNA); the cumulative length of the forked molecules ((1.84 ± 0.12) μm) was identical to that of the unforked ones. In this conventional DNA isolation process, the annealing of the complementary strands is under thermodynamic control: The most favored state is a double-stranded molecule with the most extensive base pairing. In fact, only a few molecules have bifurcated termini.

Single-stranded forms were reobtained by a process of heat denaturation followed by a rapid cooling of a very dilute solution of the purified viral DNA. In this way the renaturation process

occurs under kinetic control. Both single-stranded coiled and double-stranded forms were observed on the surface of mica (Figures 2B–E): The coils corresponded to the 88% of the molecules analyzed under the given conditions (48 molecules globally). We found bifurcated termini both in the double-stranded and in the single-stranded molecules. Most of the double-stranded molecules, contrary to the case under thermodynamic control, had one or two bifurcated termini (67%). Only a limited number of coils (31%) presented this feature.

As mentioned above, a forked double-stranded molecule is the result of coexisting intra- and intermolecular base pairing (Figure 1E). In the renatured single-stranded molecules (Figures 2C–E), the two double-stranded termini, generated by the intramolecular pairing of the terminal palindromes, can still pair with each other through the remaining short stretch of complementary bases (the white rectangles in Figure 1) to form a bifurcated terminus (Figure 1C). Their compact coiled structure is due to a high number of short base pairings involving the central 4830 bases (and possibly the termini). These single-stranded coiled forms, characterized by a high shape variability, have been termed “bush-like” by authors that obtained them under the same conditions from similar DNA.^[5]

In the single-stranded coils and in the double-stranded molecules the lengths of the arms of the forked termini were equal within measurement error ((52 ± 7) nm for the single-stranded coils and (60 ± 8) nm for the double-stranded molecules) and correspond to what is expected for the folding of the palindromic part of the termini. In a single-stranded coil, a complete pairing of the tails would produce a nonforked 130-nm-long double-stranded protrusion (Figure 1D). These longer double-stranded ends have never been observed under the experimental conditions we chose. We have seen linear tracts in 3 out of the 42 observed coiled molecules, but these tracts were significantly shorter than expected for the annealing of 383 bp: They were most likely due to the internal pairing of only one of the two termini. This experiment clearly demonstrated the tendency of the terminal palindromes to fold back.

To confirm that the formation of these double-stranded termini is driven by the sequence of the palindromes, one half of the terminal palindromes was removed by cleavage with the restriction endonuclease *Bss*HI (the location of the restriction sites is shown in Figure 1F). The cut double-stranded molecules deposited on the mica surface for SFM observation appeared to be linear, without any bifurcated terminal structures: Their mean length was (1.72 ± 0.08) μm , as expected for a double-stranded DNA molecule of 5200 bp. When a solution of these molecules was heat-denatured and then rapidly cooled, the DNA reannealed again either to form coiled single-stranded (Figure 3B) or linear double-stranded molecules (Figure 3A): In this experiment conditions were such that nearly all the molecules deposited on the surface were coiled single-strands (1074 observations). In 17% of the coils, we could identify linear straight double-stranded tracts, which had a mean length of (69 ± 12) nm (Figure 3B). These stems were due to the annealing of the incomplete terminal sequences present at both ends of the single-stranded molecules: They are still complementary to each other, even if they cannot base-pair within themselves (a

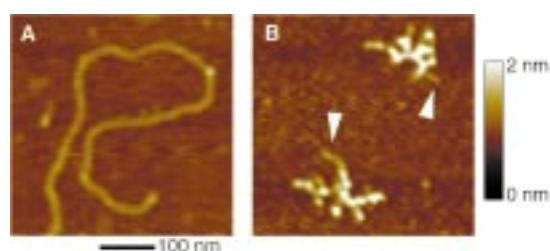


Figure 3. TM-SFM images of the B19 DNA fragment obtained after digestion with *Bss*HI, heat-denaturation and deposition onto the mica surface after reannealing. A: A detail of a molecule reannealed as a completely double-stranded form without any terminal structures. B: *Bss*HI fragments reannealed as coiled single-stranded forms. The arrows point to the putative double-stranded nonforked tail formed by the annealing of the two remaining halves of the terminal palindromes.

schematic drawing of these coiled single-stranded molecules is shown inside the dashed box of Figure 1D; the expected length of the protrusions is 68 nm). Only in a very small fraction of the coils (1.2%, 14 out of 1074) we could find structures apparently similar in shape to the forks found in the experiment performed on the complete genome. The arms of these bifurcated structures were often of different lengths; their mean length was (35 ± 8) nm, that is, considerably smaller than that found for the termini of the forks in the coils of the complete genome.

Analogous imaging experiments were performed on the single-stranded DNA of bacteriophage M13mp18 (7 kb): This led to single-stranded renatured coils with highly variable shapes not displaying any of the striking structural peculiarities observed for B19 DNA (data not shown).

In situ lysis of B19 virions: The released DNA is completely single-stranded

The experiments described above indicate that there is a strong tendency of the two terminal palindromes of the B19 single-stranded genome to fold internally and to form terminal hairpins. Nevertheless, this result does not indicate whether the viral DNA molecule inside the virion assumes this conformation. To gain information on the secondary structure of the genome molecule inside the capsid, it is necessary to avoid the sample preparation step in which the two complementary single strands of DNA can base-pair and form a double-stranded molecule. This improvement was achieved thanks to the capability of the SFM of producing meaningful data for the same specimen before and after a series of treatments, since the observation is done under mild nondestructive conditions. We performed a lysis of the B19 virions adsorbed onto the mica surface and then we inspected the area and were able to visualize the molecules released from the capsids. A spread of viral particles adsorbed on a mica surface is shown in Figure 4A. We exposed the same deposition of virions to the lytic treatment (Proteinase K and sodium dodecyl sulfate (SDS)), and inspected it again afterwards. We kept the density of virions deposited on the substrate low; consequently, the probability for single-stranded DNA molecules of one polarity to anneal to molecules

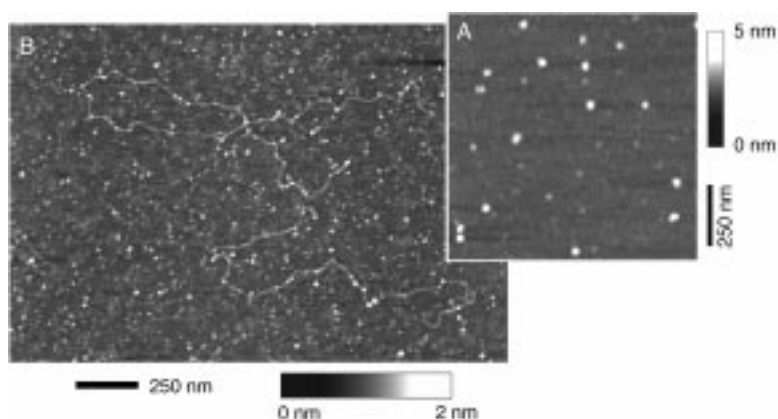


Figure 4. TM-SFM micrograph of the outcome of the *in situ* lysis experiment. A: TM-SFM image of the spread of viral particles onto the surface of freshly cleaved mica. On the surface, the round particles of smaller height (and apparent size) could be empty virions (with no DNA inside) that more easily collapse on the surface upon dehydration, or virion fragments produced by the forces involved in dehydration. B: SFM micrograph of the same surface after Proteinase K/SDS digestion *in situ*. The numerous round particles on the substrate are presumably enzyme molecules or fragments of the viral capsids not completely digested during the lysis. The localization of protein fragments of variable apparent size on the DNA can be easily seen in the SFM image. Globular protein fragments are localized on most of the imaged tails of the presumably single-stranded viral genome molecules.

of the opposite polarity to form double-stranded molecules was also low.

DNA molecules like those shown in Figure 4B were observed. They were adsorbed onto the surface of mica with a great number of objects identifiable as proteins. None of these objects were present in the spread of viral particles (Figure 4A). These proteins could be fragments of Proteinase K molecules and residual subunits of the incompletely digested viral capsids. The DNA molecules appeared to be linear and without terminal structures. The density of the DNA molecules on the surface was lower than that expected on the basis of the density of the virions that had been deposited on it (0.25 DNA molecules per μm^2 vs. 10–15 virions per μm^2). This could be partly due to the well-known presence of empty viral capsids that are erroneously counted in virion spreads, but more likely to the strong competition between proteins and DNA for the adsorption onto mica. In a control experiment we verified that SDS, at the concentration used in the *in situ* lysis experiment, did not interfere with the deposition of DNA molecules or proteins (data not shown).

The DNA molecules released from the virions had a highly variable length, ranging from 1.94 to 3.33 μm , with a mean value of $(2.33 \pm 0.6) \mu\text{m}$ (nine molecules). Single-stranded DNA is known to be very flexible and to have fewer structural constraints than double-stranded DNA, so it can be found in compact or extended conformations. In fact, while in some cases the helical rise of single-stranded DNA was measured to be as low as 2.9 Å,^[6] the length of overstretched double-stranded DNA (similar, in principle, to two facing extended nonhelical single strands in which the dihedral bond angles are not distorted) was found to be 1.7 to 2.1 times greater than that of B-DNA.^[7–9] This implies that the length of a 5600-base DNA could range from 1.6 to 4 μm , and intermediate lengths are also possible due to the

noncooperative base-stacking interaction in single-stranded DNA.^[6]

Single-stranded parvovirus DNA molecules had already been observed, for instance in the case of the minute virus of mice (MVM).^[10] These authors obtained images with an electron microscope under fully or partially denaturing conditions. The DNA molecules displayed an extended shape that is very similar to that of the molecules shown in Figure 4 of the present study. The many short double-stranded pairings that we have seen to stabilize the single-stranded coils (see above and Figures 2 and 3) were not present in the case reported in ref. [12], due to the use of formamide that denatures the double-stranded DNA.

The SFM capability to image single-stranded DNA had already been proved by Hansma et al.^[11, 12] In an experiment of partial denaturation performed on the DNA of phage λ , we could show that SFM can also distinguish between single- and double-stranded DNA tracts in the same molecule. We identified bubbles of denaturation formed by two narrow single-stranded tracts, in a prevalently double-stranded molecule (Figure 5). In the SFM image, the difference in height and width between

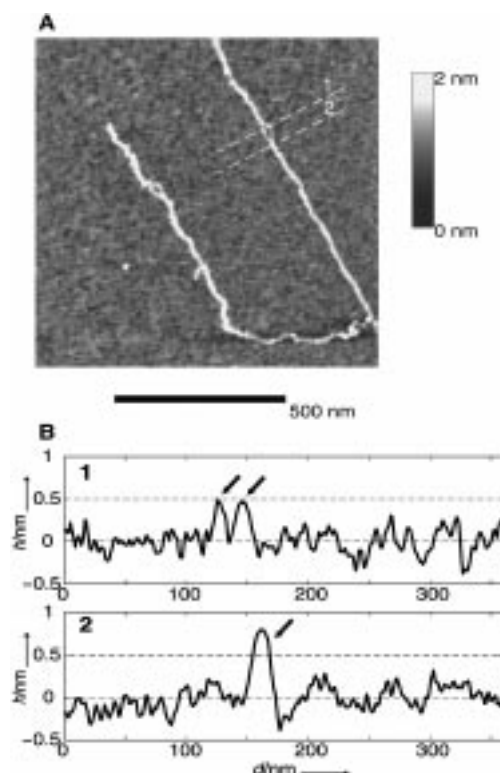


Figure 5. A: TM-SFM image of partly denatured λ phage DNA. Two uncoiled single-stranded bubbles are evident in the image. The SFM allows the unequivocal distinction between single-stranded and double-stranded DNA tracts when contemporarily present in the same image. B: Height trace of the SFM data along the lines marked in Figure 5A. The height profile displays the difference in height and width of the single-stranded and double-stranded DNA tracts (trace 1 and 2, respectively; the height peaks corresponding to the DNA strands are marked by the arrows). The height and width differences depend on the conditions of imaging and on the probe used. On the axes, h stands for the height of the features on the surface, d for the distance across it.

single- and double-stranded tracts is evident. We can therefore conclude that in none of the DNA molecules observed in our *in situ* lysis experiment double-stranded tracts were present and in particular the two palindromic termini were not folded or paired.

Is the DNA completely single-stranded also inside the capsid?

We estimated the melting temperature of a double-stranded DNA with the same base composition and length of the terminal palindromes to be approximately 60 °C at the ionic strength used in the lysis experiment.^[13] This temperature is considerably higher than that employed by us during the lysis (50 °C). We have observed normal-looking double-stranded DNA deposited on mica from a solution containing up to 0.5% (w/v) SDS, so that we can also exclude any interference of SDS with DNA base pairing (at the concentration used in our experiments; data not shown). We can therefore rule out that the base pairing in the terminal regions (or between them)—if it is already present under the conditions used for the lysis—is disrupted.

The very extended shape of the released DNA molecules, with respect to their highly compact state inside the virion, might be explained with the abrupt release of the elastic tension (entropic in nature) subsequent to the disruption of the association between the subunits of the capsid. Along their entire lengths, the adsorbed molecules do not present the short double-stranded stretches that stabilize single-stranded molecules in a coiled “bush-like” form in aqueous solution: This was expected because the experimental temperature was higher than the melting temperature of a duplex consisting of a few bases.

Double-stranded DNA is significantly more rigid than single-stranded DNA (it has a mean persistence length of 53 nm as compared to that of about 1 nm measured for single-stranded DNA^[7, 14]). In solution the two double-stranded tails should have a contour length of 62 nm and a root mean square end-to-end distance of 52 nm.^[15] Furthermore, methods of prediction of the conformation of double-stranded DNA molecules^[16, 17] did not provide us with any indication that the palindromic tails of B19 are intrinsically curved in their double-stranded state (data not shown). This is also confirmed by our images of the tails (see Figures 2 and 3). To force one or two stretches of noncurved double-stranded DNA longer than 180 bp into a capsid with an external diameter of no more than 30 nm (which must also contain all the rest of the single-stranded genome), certainly requires the assistance of very strong DNA – protein interactions, of the kind found in the nucleosome. Such very strong protein – DNA interactions have not been found by researchers in B19 or other parvoviruses.

It must be pointed out that we could reproduce the *in situ* lysis successfully only once in a number of attempts; we also tried all possible experimental variations of the successful attempt (including the exclusion of SDS) with the only result of seeing surfaces that were either perfectly clean or completely cluttered with proteins. The success rate of the experiment could not be improved due to the extreme difficulty of imaging the system at the right stage of lysis in a layer of proteins strongly competing with DNA for the adsorption onto mica. While the lysis itself should occur with a good success rate (it is indeed very

similar to the method employed to prepare soluble viral DNA), the difficulty lies in the visualization process. On the basis of the reported considerations of single- and double-stranded DNA flexibility and conformation and the findings that similar DNAs are packaged as single strands in other animal viruses,^[18] we believe that what we observed after the lytic treatment of the virions corresponds to the state of the viral DNA inside the capsid.

Structural considerations and hypotheses on the interaction of the genome with capsid proteins

The SFM image in Figure 4B shows that many proteins seem to be bound directly on the DNA strands. Proteinase K is not expected to bind to the DNA and possible residual serum proteins have not been found in SFM images of integer virions (Figure 4A), so they are assumed to be present in very small amounts. We can infer that these proteins could very well be residual (perhaps partly digested) subunits of the capsids. This would suggest an association of the viral single-stranded DNA with the capsid proteins in the virion, as has been verified for integer virions of parvoviruses from other animal sources.^[18] Such an association (not demonstrated before for B19) could help in the packaging of DNA in the viral particle when strong forces are necessary to compact a roughly 2- μ m-long DNA molecule in a shell of 20–30 nm outer diameter. Capsid formation does not itself require DNA, as empty virions are frequently found.

A stimulating hypothesis on the function of the viral proteins comes from a consideration of the energetic state of the viral genome inside the capsid. The “unfolded” structure of the termini is energetically unfavorable for the DNA sequence of the B19 genome, unless some proteins are involved in its maintenance, acting as a sort of “anti-chaperons” for DNA. A careful inspection of Figure 4B reveals that proteins seem to be distributed over the entire length of the molecules, but with a preference for the tails (there they are twice as dense as in the rest of the contour). We propose that these proteins could be helping in keeping the tails unfolded even outside the capsid (as under our condition, which were designed to be non-denaturing) and, more interestingly, inside the virion and during its assembly.

We could speculate that the unfolded state of B19 could be a requirement for easy and correct DNA packaging in the viral particle; it could also be necessary in the infection phase, for instance to facilitate entry of the DNA into the cell nucleus. As shown in this paper, the DNA alone can very easily form the terminal hairpin structures believed to be the natural substrate for DNA polymerase. It can be presumed that the viral protein – DNA interactions are disrupted inside the host cell, during the processes that lead to infection, so that the ends can fold back and become a substrate for DNA polymerase.

Conclusion

We have shown that if the B19 DNA is imaged after extraction and purification from all the proteins present in the virions, the two palindromic termini fold intramolecularly and form terminal

hairpins. On the other hand, if the viral genome is imaged at the right stage of virion lysis and prevented from interacting with DNA molecules of the opposite polarity, it appears to be completely linear and without any terminal pairings. We propose that this state of the viral genome could be maintained by an association between the DNA and capsid proteins. Our experiment on the in situ lysis of single virions of B19 measured conformational properties not accessible to date with any other analytical techniques.

The analysis conducted on renatured single-stranded molecules singled out peculiar structural features from the apparently random structure of the coiled molecules. The structural regularity of the bifurcated double-stranded termini found in our experiments for the coiled single-stranded molecules, whose three-dimensional shape is a complex result of the kinetics of renaturation, is astonishing. The local loss of entropy (due to the high stability of the extended duplexes at the termini of the B19 DNA) creates a structurally distinguished feature in the coils. The microscope analysis can localize this feature very efficiently in single molecules, even if conditions are such that only a fraction of the population displays it. This analytical strategy could very well be used for other structural/topological determinations where relatively small and very local structural regularities could be highlighted, even if evident only in a fraction of the molecules.

Experimental Section

SFM imaging of B19 virions and of native and denatured B19 DNA: A B19 viremic serum sample was obtained from an experimental infection in a human volunteer and was used as a source of virus for molecular studies. B19 virus was purified from serum by centrifugation through a cushion of 30% glycerol in STE buffer (150 mM NaCl, 10 mM Tris-HCl, pH 7.5, 1 mM EDTA) at 40000 g and 4 °C for 4 h. Pelleted virions were resuspended in STE buffer. Virions were lysed by incubation with 100 µg mL⁻¹ Proteinase K, 1% (w/v) SDS at 50 °C for 2 h. Viral DNA was purified by adsorption onto QIAEX silica matrix (Qiagen, Hilden, Germany) following manufacturer's instructions and eluted in TE buffer (10 mM Tris-HCl, pH 7.5, 1 mM EDTA) as annealed double-stranded DNA.

Native B19 virions and purified DNA molecules were deposited on freshly cleaved ruby mica (B&M Mica Co. Inc., New York, NY) from a nanomolar DNA solution containing 4 mM HEPES buffer (pH 7.4), 10 mM NaCl, 2 mM MgCl₂ (HEPES = 2-[4-(2-hydroxyethyl)-1-piperazinyl]ethanesulfonic acid). The Mg²⁺ ions are added to promote DNA adsorption on mica.^[19, 20] 10–15 µL of DNA solution were deposited on a 1–1.5 cm² mica disc and left there for approximately 1 min, then rinsed with 2–3 mL of milliQ-deionized water (Millipore, USA), which was added dropwise, and dried under a gentle flow of nitrogen gas.

Imaging was performed in tapping mode with PointProbe non-contact silicon probes (NanoSensors, Germany) on a NanoScope IIIa scanning force microscope system equipped with a multimode head and a type E piezoelectric scanner (Digital Instruments, Santa Barbara, CA, USA). Images were recorded with a 10–15 µm linear scanning speed at a sampling density of 4–9 nm² per pixel.

Heat denaturation of double-stranded purified B19 DNA was performed on the diluted specimens prepared for imaging. After 1 min at 95 °C the specimens were quickly cooled (on ice) and spread onto freshly cleaved mica in the same way as native DNA specimens.

Lysis on the mica surface: B19 virion spreads on mica (obtained as described above) were subjected to SFM analysis to check for the density of deposition. The spreads were treated with a solution containing 10 µg mL⁻¹ Proteinase K, 0.1% (w/v) SDS in 4 mM HEPES buffer (pH 7.4) at 50 °C for 10 min, rinsed with milliQ-deionized water, dried with nitrogen, and observed with the SFM.

Imaging of partially denatured DNA molecules: Partially denatured λ phage DNA molecules were obtained by adding 10% formaldehyde to the diluted 4 mM HEPES buffer (pH 7.4), 10 mM NaCl, 2 mM MgCl₂ solution used for deposition on mica (modified from ref. [21]). The solutions were kept for 10 min at 65 °C and then cooled on ice for 10 min. The formaldehyde-containing DNA solution was deposited on freshly cleaved mica as described above for the other specimens and imaged with the SFM.

Image processing and molecule measurements: Raw SFM images were processed only for background removal (flattening) using the microscope manufacturer's image-processing software. DNA molecule lengths were measured from the SFM images using ALEX, a software package written for probe microscopy image processing.^[22]

We are grateful to Prof. Ernesto Di Mauro (Univ. La Sapienza, Rome, Italy) for very helpful discussions. This work was supported by Programmi Biotecnologie Legge 95/95 (MURST 5%); MURST PRIN (Progetti Biologica Strutturale 1997–1999 and 1999–2001) (G.Z., A.B., and B.S.) and by CNR target project on "Biotechnology" and MURST (G.G. and M.M.).

- [1] J. Mori, P. Beattie, D. W. Melton, B. J. Cohen, J. P. Clewley, *J. Gen. Virol.* **1987**, *68*, 2797–2806, and references therein.
- [2] G. Binnig, C. F. Quate, C. Gerber, *Phys. Rev. Lett.* **1986**, *56*, 930–933.
- [3] C. Bustamante, C. Rivetti, D. J. Keller, *Curr. Opin. Struct. Biol.* **1997**, *7*, 709–716.
- [4] C. Bustamante, D. Keller, *Physics Today* **1995**, *48*, 32–38.
- [5] C. F. Garon, E. Barbosa, B. Moss, *Proc. Natl. Acad. Sci. USA* **1978**, *75*, 4863–4867.
- [6] W. Saenger, *Principles of Nucleic Acid Structure*, Springer, New York, **1984**.
- [7] S. B. Smith, Y. Cui, C. Bustamante, *Science* **1996**, *271*, 795–799.
- [8] D. Bensimon, A. J. Simon, V. Croquette, A. Bensimon, *Phys. Rev. Lett.* **1995**, *74*, 4754–4757.
- [9] T. Thundat, D. P. Allison, R. J. Warmack, *Nucleic Acids Res.* **1994**, *22*, 4224–4228.
- [10] G. J. Bourguignon, P. J. Tattersall, D. C. Ward, *J. Virol.* **1976**, *20*, 290–306.
- [11] H. G. Hansma, R. L. Sinsheimer, M. Q. Li, P. K. Hansma, *Nucleic Acids Res.* **1992**, *20*, 3585–3590.
- [12] H. G. Hansma, I. Revenko, K. Kim, D. E. Laney, *Nucleic Acids Res.* **1996**, *24*, 713–720.
- [13] C. R. Cantor, P. R. Schimmel, *Biophysical Chemistry, Vol. 3*, Freeman, San Francisco, **1980**.
- [14] C. Rivetti, C. Walker, C. Bustamante, *J. Mol. Biol.* **1998**, *280*, 41–59.
- [15] C. Frontali, E. Dore, A. Ferrauto, E. Gratton, A. Bettini, M. R. Pozzan, E. Valdevit, *Biopolymers* **1979**, *18*, 1353–1373.
- [16] C. Anselmi, G. Bocchinfuso, P. De Santis, M. Savino, A. Scipioni, *J. Mol. Biol.* **1999**, *286*, 1293–1301.
- [17] E. S. Shpigelman, E. N. Trifonov, A. Bolshoy, *Comput. Appl. Biosci.* **1993**, *9*, 435–440.
- [18] M. S. Chapman, M. G. Rossmann, *Structure* **1995**, *3*, 151–162.
- [19] C. Bustamante, J. Vesenka, C. L. Tang, W. Rees, M. Guthold, R. Keller, *Biochemistry* **1992**, *31*, 22–26.
- [20] M. Bezanilla, S. Manne, D. E. Laney, Y. L. Lyubchenko, H. G. Hansma, *Langmuir* **1995**, *11*, 655–659.
- [21] R. B. Inman, *J. Mol. Biol.* **1967**, *28*, 103–116.
- [22] C. Rivetti, M. Guthold, C. Bustamante, *J. Mol. Biol.* **1996**, *264*, 919–932.

Received: May 9, 2000

Revised version: September 18, 2000 [F 62]